



Dynamical Mechanism for Coexistence of Dispersing Species

MARY ANN HARRISON*†, YING-CHENG LAI‡ AND ROBERT D. HOLT§

*Department of Physics and Astronomy, The University of Kansas, Lawrence, KS 66045, U.S.A.,
‡Departments of Mathematics, Electrical Engineering, and Physics, Center for Systems Science and
Engineering Research, Arizona State University, Tempe, AZ 85287, U.S.A. and §Department of Zoology,
University of Florida, Gainesville, FL 32611, U.S.A.

(Received on 9 November 2000, Accepted in revised form on 19 July 2001)

Dispersal of organisms may play an essential role in the coexistence of species. Recent studies of the evolution of dispersal in temporally varying environments suggest that clones differing in dispersal rates can coexist indefinitely. In this work, we explore the mechanism permitting such coexistence for a model of dispersal in a patchy environment, where temporal heterogeneity arises from endogenous chaotic dynamics. We show that coexistence arises from an extreme type of intermittent behavior, namely the phenomenon known as on-off intermittency. In effect, coexistence arises because of an alternation between synchronized and de-synchronized dynamical behaviors. Our analysis of the dynamical mechanism for on-off intermittency lends strong credence to the proposition that chaotic synchronism may be a general feature of species coexistence, where competing species differ only in dispersal rate.

© 2001 Academic Press

1. Introduction

Understanding the factors that promote or prevent the coexistence of competing species is a topic which has long been central to community ecology (Hutchinson, 1978; Roughgarden & Diamond, 1986; Tokeshi, 1999). Traditional approaches to coexistence emphasize niche partitioning, defined broadly to include differentiation in response to predators and parasites as well as differentiation in resource use (Holt *et al.*, 1994). Such partitioning permits different species to experience different limiting factors at the spatial scale of local communities. Recent years have seen a growing appreciation of the importance of spatial heterogeneity and dispersal in explaining

species coexistence (Hanski, 1999). The coexistence of species in local communities may thus reflect how communities are coupled in space. One familiar mechanism by which dispersal facilitates coexistence at the landscape scale is a trade-off among species between colonizing and competitive abilities (Lehman & Tilman, 1997). For instance, consider a guild of competitors that utilizes a single limiting resource. In a closed, local habitat patch, the species which can persist at the lowest resource level will eventually displace species with higher resource requirements (Grover, 1997). However, if habitat patches are open, and if there are spatially asynchronous extinctions that deplete patches, rapidly dispersing, yet inferior competitors may be able to coexist regionally with superior competitors. In effect, rapid dispersal can provide temporary windows of opportunity during which inferior

† Author to whom correspondence should be addressed.
Current address: Flint Hills Scientific, L.L.C., 5020W 15th St., Suite A, Lawrence, KS 66049. E-mail: mafh@fhs.lawrence.ks.us

competitors can colonize empty patches. There, they reproduce sufficiently fast to colonize yet other patches before being excluded by species that are more slowly dispersing, but competitively superior.

Studies of the evolution of dispersal have revealed another mechanism by which dispersal can influence species coexistence. Factors favoring the evolution of dispersal include competition among kind and inbreeding effects (Hamilton & May, 1997; Comins, 1982; Taylor, 1988; Wiener & Feldman, 1991), the interplay of within-population and between-population selection (Kuno, 1981; Olivieri *et al.*, 1995), and spatiotemporal variation in fitness arising from environmental variability (Gadgil, 1971; Roff, 1975; Metz *et al.*, 1983; Levin *et al.*, 1984; Cohen & Levin, 1991). Without temporal variation, spatial heterogeneity alone does not tend to favor the evolution of dispersal (Hastings, 1983; Holt, 1985). Recently, it has been recognized that even if the external environment is constant, nonlinear population dynamics leading to cycles or chaotic dynamics can produce the appropriate spatiotemporal variation in fitness that favors the evolution of dispersal (Holt & McPeek, 1996; Doebeli & Ruxton, 1997; Parvinen, 1999). In these theoretical studies, it is assumed that clones compete in patches and disperse among patches. Within patches, all clones are equivalent, but clones may differ in their rates of movement among patches. An intriguing pattern which has emerged in these studies is that given unstable dynamics, there is sustained coexistence of two or more clones differing in dispersal rates. This coexistence is permanent (Law, 1999) in that each clonal species can increase when it is rare and the other species is in its single-species dynamical attractor.

Since these models assume that clones behave identically within patches (so that density dependence is experienced uniformly within and among clones), there is by definition no tradeoff between colonizing and competitive abilities. Holt & McPeek (1996) conjectured that coexistence arises because the system tends to shift between distinct dynamical behaviors concordant with temporal variation in average dispersal rates. For instance, at high dispersal rates, different habitats tend to become synchronized in their dynamics. This favors low dispersal, if there is

spatial variance in fitness (Hastings, 1983). However, as the system evolves towards lower dispersal rates, the dynamics of different patches become de-synchronized, and a selective advantage of dispersal then emerges.

In this paper, we attempt to articulate this conjecture in more detail, and in particular to examine the dynamical mechanism responsible for the coexistence of competing dispersing clones. Our analysis and numerical experiments suggest a mechanism whereby the temporal synchronization and de-synchronization between populations in different habitats occurs in an intermittent fashion.

We consider a simple system consisting of two patches and two clones, with N_{t1} and N_{t2} being the total populations in patches 1 and 2, respectively. Then, the relative populations of the two patches, defined to be the ratios between N_{t1}/K_1 and N_{t2}/K_2 , tend to be approximately equal in long epochs of time (known as laminar phases). The synchronization is, however, interrupted by time periods in which the relative populations deviate rapidly from each other in sudden bursts. The deviation occurs randomly in time and typically lasts for a short time period (compared with the average time duration of the laminar phase), after which temporal synchronization between the relative population is restored. Thus, if we define the following quantity to characterize the quality of synchronization:

$$Q(t) = \frac{N_{t1}(t)}{K_1} - \frac{N_{t2}(t)}{K_2}, \quad (1)$$

then $Q(t)$ exhibits on-off intermittency, a dynamical behavior that has received extensive recent attention (Spiegel, 1980; Fujisaka & Yamada, 1985, 1986; Fujisaka *et al.*, 1986; Yu *et al.*, 1991; Platt *et al.*, 1993; Heagy *et al.*, 1994; Lai & Grebogi, 1995; Lai, 1996a, b; Yalcinkaya & Lai, 1996; Venkataramani *et al.*, 1995, 1996; Marthaler *et al.*, 2001). In ecology, Ferriere & Cazelles (1999) recently observed that on-off intermittency describes the dynamics of many natural populations, where variable periods of time at low rarity alternate with sudden outbreaks. They show that such intermittency can arise from different models of competition, where coexistence

arises because of a local storage effect (Chesson, 1986). However, we demonstrate here that on-off intermittency characterizes a competition model where coexistence arises from *dispersal* among patches. Our analysis of the intermittent mechanism suggests that the coexistence is unlikely to be a transient behavior. An implication is that intermittently chaotic synchronism may represent a contributing dynamical mechanism for the coexistence of competing species in spatially extended ecological systems.

This paper is organized as follows. In Section 2, we describe the Holt–McPeek model. In section 3, we review the theory of synchronous chaos and on-off intermittency. In Section 4, we present a detailed numerical analysis of the Holt–McPeek model, demonstrating the prevalence of synchronous chaos with on-off intermittency. A discussion is presented in Section 5. In Appendix A, we construct a simplified version of the Holt–McPeek model, which allows for partial physical analysis, to better understand the dynamical origin of chaotic synchronization and on-off intermittency in ecological systems.

2. The Holt–McPeek Model

Holt and McPeek consider a population model of two clones that could occupy two different local patches. The model is a generalization of the well-known Ricker model that involves two patches (May & Oster, 1976). The density of clone i , in patch j at generation t is $N_{ij}(t)$. The local population growth rate, or the realized fitness, of clone i in patch j is given by

$$W_j(t) = \exp \left[r_j \left(1 - \frac{N_{1j}(t) + N_{2j}(t)}{K_j} \right) \right], \quad (2)$$

where r_j is the intrinsic rate of increase at low-population size in patch j and K_j the carrying capacity of patch j . The model assumes that the growth rate is identical for each clone within each patch ($r_{1j} = r_{2j} = r_j$), and that the carrying capacity K_j depends on the total population in the patch.

To model dispersal, Holt and McPeek assume that of the total population of clone i , a fraction e_i migrate at each generation from their natal patch, while the remainder ($1 - e_i$) remain in this

patch. The quantity e_i is then the dispersal rate of clone i . We assume that this quantity differs between clones, though they are identical in all other respects. The migratory fraction of the population experiences a mortality rate, or cost of dispersal, of $(1 - m)$, leaving only a fraction m of immigrants to compete on equal terms with the resident population. The resulting model, illustrated schematically in Fig. 1, assumes that reproduction and density dependence precedes dispersal. The census immediately follows dispersal, costs of dispersal for a clone are experienced entirely by those individuals who actually disperse, and population densities are sufficiently high so that they can be represented by continuous variables rather than discrete integers. The complete model is then as follows:

$$\begin{aligned} N_{11}(t+1) &= (1 - e_1) W_1 [N_{t1}(t)] N_{11}(t) \\ &\quad + me_1 W_2 [N_{t2}(t)] N_{12}(t), \\ N_{12}(t+1) &= (1 - e_1) W_2 [N_{t2}(t)] N_{12}(t) \\ &\quad + me_1 W_1 [N_{t1}(t)] N_{11}(t), \\ N_{21}(t+1) &= (1 - e_2) W_1 [N_{t1}(t)] N_{21}(t) \\ &\quad + me_2 W_2 [N_{t2}(t)] N_{22}(t), \\ N_{22}(t+1) &= (1 - e_2) W_2 [N_{t2}(t)] N_{22}(t) \\ &\quad + me_2 W_1 [N_{t1}(t)] N_{21}(t). \end{aligned} \quad (3)$$

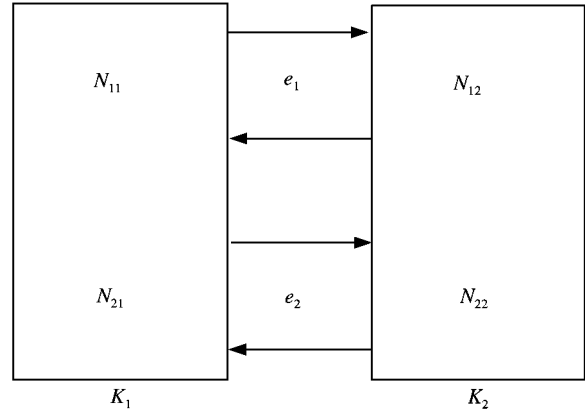


FIG. 1. Schematic diagram of the Holt–McPeek model consisting of two different clones which can exist in two different patches.

Holt and McPeek study this model at the extreme ends of dispersal: one clone with a low dispersal rate ($e_1 = 0.01$) competing with another clone with a high dispersal rate ($e_2 = 0.5$). At low values of $r = r_1 = r_2$ (the intrinsic growth rate), the system experiences stable or cyclic dynamics. As a consequence, dispersal is disfavored, with the high-dispersal clone asymptotically decaying to a zero population size. This is consistent with previous findings that spatial heterogeneity alone is insufficient to promote the coexistence of species differing only in dispersal (Hastings, 1983; Holt, 1985; Liberman & Feldman, 1989). The reason is that if habitats vary in their carrying capacities, initially, the populations in the high- K patch are larger than those in the low- K patch. Now, consider the dispersing species. For a fixed dispersing rate, there is then an asymmetric flow of individuals from high- K to low- K patches, depressing fitness in the low- K patch, and increasing fitness in the high- K patch. Due to the low fitness, certain individuals will die off in the low- K patch, leading to a constant relative abundance of the population in the high- K patch and hence, a constant flow of the population of the low- K patch. If there is no temporal variation in the fitness, this flow will continue until the dispersing populations die off completely. Thus, in spatially heterogeneous but temporally homogeneous environments, dispersal is disfavored. Temporal heterogeneity is thus required for the coexistence of species of dramatically different dispersal rates. At higher values of r , the model experiences a transition to chaos, which then provides the temporal heterogeneity required for coexistence.

As an example, using the parameter values: $K_1 = 100$, $K_2 = 50$, $e_1 = 0.5$, $e_2 = 0.01$, $m = 1$, and $r_1 = r_2 = r$, Holt and McPeek find that low r values of 1 and 2.5 produce stable and cyclic dynamics, respectively. Given population stability, clones with relatively lower dispersal rates (i.e. $e_2 = 0.01$) displace clones with higher dispersal rates (i.e. $e_1 = 0.5$). With the high-dispersal clone now extinct, the average dispersal rate of the population is low. In other words, dispersal is disfavored. However, for the higher r value of 3.0, a chaotic behavior arises: instead of dying off, the high dispersal clone now persists, and experiences episodic increases in population, as shown in

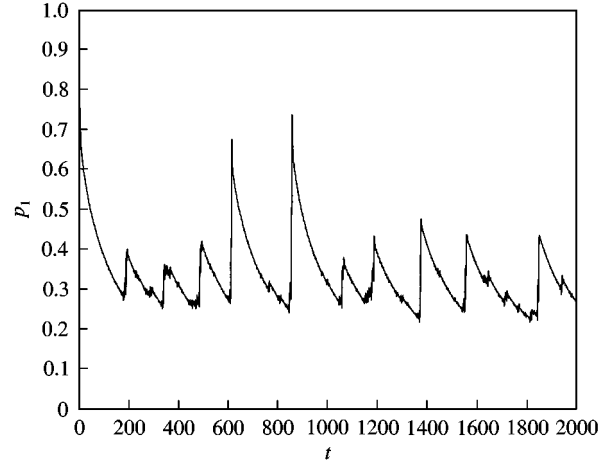


FIG. 2. Time series $P_1(t)$ for Holt–McPeek model with $r = 3.0$, $K_1 = 100$, $K_2 = 50$, $e_1 = 0.5$, $e_2 = 0.01$, and $m = 1$.

Fig. 2, where the time trace of the frequency of the high dispersal clone, defined to be

$$p_1(t) = \frac{N_{11}(t) + N_{12}(t)}{N_{11}(t) + N_{12}(t) + N_{21}(t) + N_{22}(t)}$$

is plotted. Holt and McPeek conclude, based on this observation, that *chaos favors dispersal*. We also note that the increase of $p_1(t)$ is sudden and fast but the decline (relaxation) is relatively slow, which, as we will argue in Section 4, can be explained based on on-off intermittency.

How likely is the presence of coexistence due to this mechanism in the Holt–McPeek model? To address this question, we numerically study the parameter space and examine whether the parameter regions for chaos are appreciable. There are three parameters in the Holt–McPeek model: r , e_1 , and e_2 . Thus, we fix a few values of r and explore the two-dimensional parameter plane formed by e_1 and e_2 . The results are shown in Fig. 3(a–c), which are produced by choosing a grid of 500×500 parameter pairs in the region ($0 \leq e_1 \leq 0.5$, $0 \leq e_2 \leq 0.5$) and computing, for each parameter pair, the time-average value of the frequency of the high-dispersal clone $p_1(t)$ for 10^4 iterations of eqn (3), after discarding an initial transient of 10^3 iterations. The value of p_1 is represented by the color of the (e_1, e_2) point: dark points correspond to $p_1 = 0$ or $p_1 = 1$ (extinction of one clone), while gray points

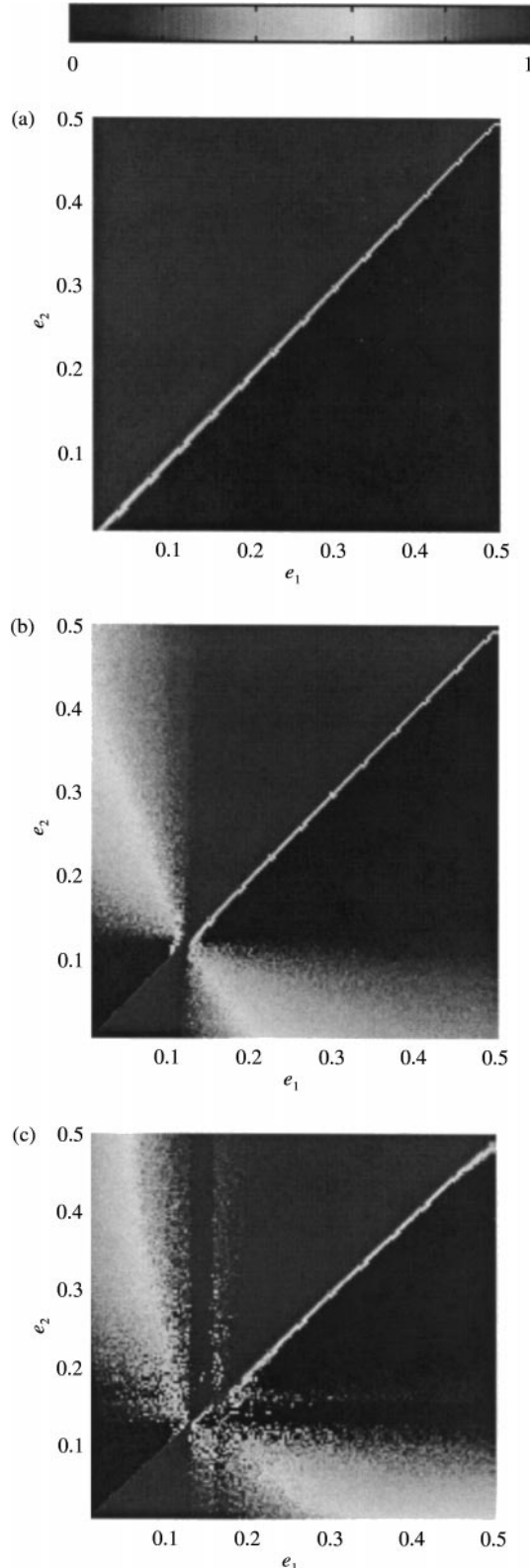


FIG. 3. Average frequency of the high-dispersal clone (p_1) calculated over 10^4 iterates after discarding an initial 10^3 for (a) $r = 2.0$, (b) $r = 3.0$, and (c) $r = 4.0$.

represent p_1 near 0.5 (coexistence), with the lightness changing continuously for intermediate values, as indicated at the top of the figure. When r is low, as in Fig. 3(a), where $r = 2.0$, we see that one of the two clones becomes extinct for all values of (e_1, e_2) except when $e_1 \approx e_2$, on the diagonal of the figure. However, as r is increased, as in Fig. 3(b) and (c), large parameter ranges exist where there is coexistence of the two species. Furthermore, we find that in this same region, the model is chaotic in that the system has at least one positive Lyapunov exponent. Thus, the phenomenon (that chaos favors dispersal) is typical in the sense that it can occur in large regions in the parameter space.

Based on their numerical observations, Holt and McPeek argue that there are two qualitatively distinct states in the chaotic regime:

1. The populations in the two patches tend to be synchronized when the frequency of the high-dispersal clone (p_1) is large because there is a strong coupling between the two patches. In this nearly synchronized state, dispersal becomes disadvantageous, leading to a decrease in p_1 and hence, over time, the patch dynamics become progressively decoupled.

2. As a consequence of the reduced coupling strength, the approximate synchronization state can no longer be maintained, so the patch populations become desynchronized and dispersal becomes advantageous again, thereby pushing the system towards synchronization.

This scenario: synchronization \rightarrow de-synchronization \rightarrow synchronization $\rightarrow \dots$, with random time intervals between stages of de-synchronization, is a characteristic dynamical pattern of on-off intermittency.

3. Theory of Synchronous Chaos and On-off Intermittency

To gain insight into the intermittent dynamics in the ecological model, we first review, in a general setting, how synchronous chaos and on-off intermittency can arise in linearly coupled maps. We caution that ecological models, such as eqn (3), are usually represented by nonlinearly coupled, non-identical chaotic maps, which in

general cannot be reduced to linearly coupled maps. The study of linearly coupled maps, nonetheless, serves the purposes of introducing notations and understanding the basic dynamics of synchronization that can occur in more complicated ecological models. Based on the study of linearly coupled maps, we will attempt to provide a *qualitative* theory on how intermittent synchronization can occur and sustain in a model of dispersal described by nonlinearly coupled, non-identical chaotic maps.

3.1. LINEARLY COUPLED MAPS

We consider the following general system of two-coupled chaotic maps:

$$\begin{aligned} \mathbf{x}_{n+1} &= \mathbf{f}_1(\mathbf{x}_n) + \mathbf{C} \cdot (\mathbf{y}_n - \mathbf{x}_n), \\ \mathbf{y}_{n+1} &= \mathbf{f}_2(\mathbf{y}_n) + \mathbf{C} \cdot (\mathbf{x}_n - \mathbf{y}_n), \end{aligned} \quad (4)$$

where \mathbf{x} and \mathbf{y} are the N -dimensional vectors ($\mathbf{x} \in \mathcal{R}^N$ and $\mathbf{y} \in \mathcal{R}^N$), \mathbf{f}_1 and \mathbf{f}_2 are the nonlinear maps that can generate chaos, and \mathbf{C} is the $N \times N$ coupling matrix. We stress that realistic ecological models, such as the Holt–McPeek model equation (3), are in general more complicated than eqn (4). Nonetheless, the phenomenon of chaotic synchronization can be conveniently addressed by eqn (4).

If the maps are identical, i.e. $\mathbf{f}_1 = \mathbf{f}_2 \equiv \mathbf{f}$, then the synchronization state, defined by $\mathbf{x}_n = \mathbf{y}_n$, is a solution of eqn (4). In mathematical terms, we say the solution $\mathbf{x}_n = \mathbf{y}_n$ lives on the N -dimensional synchronization manifold, denoted by \mathcal{M} . \mathcal{M} is an *invariant* manifold in the full $2N$ -dimensional phase space because a trajectory starting with an initial condition on \mathcal{M} , i.e. $\mathbf{x}_0 = \mathbf{y}_0$, lies in \mathcal{M} forever: $\mathbf{x}_n = \mathbf{y}_n$ for all $n \geq 1$. Since \mathcal{M} is only a subspace in the full phase space, whether synchronization can be achieved for randomly chosen initial conditions depends on the stability of \mathcal{M} with respect to perturbations *transverse* to \mathcal{M} . In particular, if \mathcal{M} is transversely stable, a trajectory in the vicinity of \mathcal{M} will approach \mathcal{M} exponentially, leading to physically observable synchronization. However, if \mathcal{M} is transversely unstable, a perturbation in the transverse subspace will be amplified exponentially and a trajectory cannot stay near \mathcal{M} indefinitely;

therefore, though \mathcal{M} is invariant, the synchronization state is not physically observable.

To quantify the stability of the synchronization manifold \mathcal{M} , we examine the evolution of an infinitesimal vector transverse to \mathcal{M} . For convenience, we make use of the following change of variables:

$$\mathbf{u} = \frac{\mathbf{x} + \mathbf{y}}{2}, \quad \mathbf{v} = \frac{\mathbf{x} - \mathbf{y}}{2} \quad (5)$$

or

$$\mathbf{x} = \mathbf{u} + \mathbf{v}, \quad \mathbf{y} = \mathbf{u} - \mathbf{v}. \quad (6)$$

Clearly, \mathbf{u} and \mathbf{v} are the dynamical variables *in* and *transverse* to \mathcal{M} , respectively, as shown schematically in Fig. 4. To derive maps for the new variables \mathbf{u} and \mathbf{v} , we substitute eqn (4) into eqn (5) to obtain

$$\begin{aligned} \mathbf{u}_{n+1} &= \frac{1}{2}(\mathbf{x}_{n+1} + \mathbf{y}_{n+1}) = \frac{1}{2}[\mathbf{f}(\mathbf{x}_n) + \mathbf{f}(\mathbf{y}_n)] \\ &= \frac{1}{2}[\mathbf{f}(\mathbf{u}_n + \mathbf{v}_n) + \mathbf{f}(\mathbf{u}_n - \mathbf{v}_n)], \\ \mathbf{v}_{n+1} &= \frac{1}{2}(\mathbf{x}_{n+1} - \mathbf{y}_{n+1}) = \frac{1}{2}[\mathbf{f}(\mathbf{u}_n + \mathbf{v}_n) \\ &\quad - \mathbf{f}(\mathbf{u}_n - \mathbf{v}_n) - 4\mathbf{C} \cdot \mathbf{v}_n]. \end{aligned} \quad (7)$$

Since we are interested in the dynamics near the synchronization manifold in which \mathbf{v}_n is

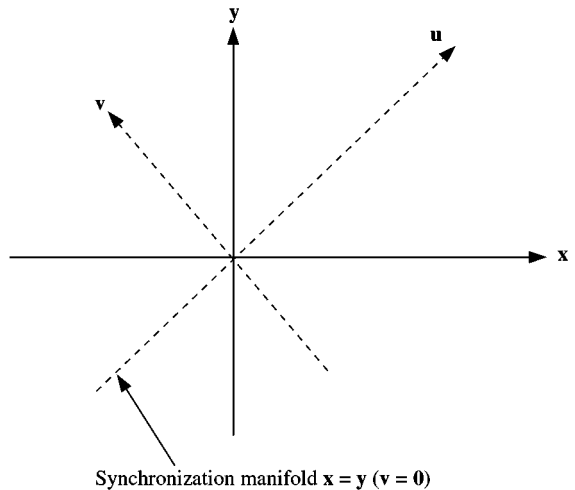


FIG. 4. Schematic illustration of the relation between the variables (\mathbf{x}, \mathbf{y}) and (\mathbf{u}, \mathbf{v}) , where $\mathbf{v} = \mathbf{0}$ denotes the synchronization manifold.

infinitesimally small: $|\mathbf{v}_n| \approx \mathbf{0}$ ($|\mathbf{v}_n|$ is the length of the vector \mathbf{v}_n), we can approximate the functions $\mathbf{f}(\mathbf{u}_n \pm \mathbf{v}_n)$ to first order in \mathbf{v}_n by utilizing the Taylor expansions. That is, in the Taylor series of $\mathbf{f}(\mathbf{u}_n \pm \mathbf{v}_n)$, we neglect terms containing derivatives of the vector function \mathbf{f} of orders higher than one. We obtain

$$\mathbf{f}(\mathbf{u}_n \pm \mathbf{v}_n) \approx \mathbf{f}(\mathbf{u}_n) \pm \frac{\partial \mathbf{f}}{\partial \mathbf{w}} \Big|_{\mathbf{v}_n = \mathbf{0}} \cdot \mathbf{v}_n, \quad (8)$$

where $\partial \mathbf{f} / \partial \mathbf{w}|_{\mathbf{v}_n = \mathbf{0}}$ stands for the first-order derivatives of \mathbf{f} with respect to its argument $\mathbf{w}_n \equiv \mathbf{u}_n \pm \mathbf{v}_n$, evaluated at $\mathbf{v}_n = \mathbf{0}$. Note that, since \mathbf{f} is a vector function, the first-order derivative of \mathbf{f} is in fact a matrix, the *Jacobian matrix*. In terms of the vector components: $\mathbf{w} = \{w_1, w_2, \dots, w_N\}$, and $\mathbf{f}(\mathbf{w}) = \{f_1(\mathbf{w}), f_2(\mathbf{w}), \dots, f_N(\mathbf{w})\}$, the Jacobian matrix is given by

$$\mathbf{J} \equiv \frac{\partial \mathbf{f}}{\partial \mathbf{w}} = \begin{pmatrix} \frac{\partial f_1}{\partial \omega_1} & \frac{\partial f_1}{\partial \omega_2} & \dots & \frac{\partial f_1}{\partial \omega_N} \\ \frac{\partial f_2}{\partial \omega_1} & \frac{\partial f_2}{\partial \omega_2} & \dots & \frac{\partial f_2}{\partial \omega_N} \\ \dots & \dots & \dots & \dots \\ \frac{\partial f_N}{\partial \omega_1} & \frac{\partial f_N}{\partial \omega_2} & \dots & \frac{\partial f_N}{\partial \omega_N} \end{pmatrix}. \quad (9)$$

Since the Jacobian matrix is evaluated at $\mathbf{v}_n = \mathbf{0}$, it depends on \mathbf{u}_n only. We write $\mathbf{J}(\mathbf{u}_n)$. By substituting eqn (8) into eqn (7), we obtain

$$\begin{aligned} \mathbf{u}_{n+1} &\approx \mathbf{f}(\mathbf{u}_n), \\ \mathbf{v}_{n+1} &\approx [\mathbf{J}(\mathbf{u}_n) - 2\mathbf{C}] \cdot \mathbf{v}_n. \end{aligned} \quad (10)$$

Equation (10) thus represents a unidirectionally coupled system between the dynamical variables \mathbf{u} and \mathbf{v} in the sense that the \mathbf{v} -dynamics does not influence that of \mathbf{u} . Moreover, the \mathbf{u} -dynamics is completely determined by the original map \mathbf{f} . The spectrum of N Lyapunov exponents of the \mathbf{u} -dynamics is then determined by

$$\begin{aligned} \lambda^j &= \lim_{L \rightarrow \infty} \frac{1}{L} \sum_{n=0}^{L-1} \ln \frac{|\mathbf{u}_{n+1}|}{|\mathbf{u}_n|} = \lim_{L \rightarrow \infty} \frac{1}{L} \sum_{n=0}^{L-1} \\ &|(\mathbf{J}(\mathbf{u}_n)) \cdot \overline{\mathbf{u}}_n^j|, \quad j = 1, \dots, N, \end{aligned} \quad (11)$$

where $\{\overline{\mathbf{u}}_n^1, \dots, \overline{\mathbf{u}}_n^N\}$ is a set of orthonormal unit vectors at the trajectory point \mathbf{u}_n in the \mathbf{u} space. Since $\mathbf{f}(\mathbf{u})$ is chaotic, some of the Lyapunov exponents are positive. Equation (10) can also be regarded as a driving-driven system, where the chaotic variable \mathbf{u} , generated by the chaotic dynamics in the synchronization manifold \mathcal{M} , drives the variable in the transverse subspace \mathcal{T} . The transverse stability of the chaotic trajectory in \mathcal{M} is then determined by the matrix: $[\mathbf{J}(\mathbf{u}) - 2\mathbf{C}]$. Also, note that the map of \mathbf{v} is linear with a fixed point $\mathbf{v} = \mathbf{0}$ that corresponds to the synchronization state between the original dynamical variables \mathbf{x} and \mathbf{y} . Thus, if there is no coupling, i.e. $\mathbf{C} = \mathbf{0}$, the Lyapunov spectrum of \mathbf{v} -dynamics is the same as that of the \mathbf{u} -dynamics, so the fixed point $\mathbf{v} = \mathbf{0}$ is unstable, which means that the synchronization manifold is transversely unstable and thus cannot be realized physically. As the coupling is increased, the matrix $[\mathbf{J}(\mathbf{u}) - 2\mathbf{C}]$ becomes less unstable until when the coupling exceeds a critical value, after which, all Lyapunov exponents generated by the matrix (also called the *transverse Lyapunov exponents*) become negative so that the synchronization state $\mathbf{v} = \mathbf{0}$ becomes stable. In particular, the transverse Lyapunov spectrum can be defined as follows:

$$\begin{aligned} \Lambda_j^T &= \lim_{L \rightarrow \infty} \frac{1}{L} \sum_{n=0}^{L-1} \ln \frac{|\mathbf{v}_{n+1}|}{|\mathbf{v}_n|} \\ &= \lim_{L \rightarrow \infty} \frac{1}{L} \sum_{n=0}^{L-1} |(\mathbf{J}(\mathbf{u}_n) - 2\mathbf{C}) \cdot \overline{\mathbf{v}}_n^j|, \end{aligned} \quad (12)$$

where $\{\overline{\mathbf{v}}_n^1, \dots, \overline{\mathbf{v}}_n^N\}$ is a set of orthonormal unit vectors in the \mathbf{v} space that evolve with time. Arrange the N transverse Lyapunov exponents in the following order: $\Lambda_1^T \geq \Lambda_2^T \geq \dots \geq \Lambda_N^T$. When there is no coupling, the transverse Lyapunov spectrum coincides with that of the chaotic map \mathbf{f} . Synchronization can be physically realized when the largest transverse Lyapunov exponent becomes negative. We remark that synchronization of more than two-coupled chaotic maps (or continuous-time flows) can be formulated in a similar way (Pecora & Carroll, 1998).

What if the synchronization manifold is weakly unstable in the transverse space, i.e. when Λ_1^T is slightly positive? Since Λ_1^T is an asymptotic

quantity, i.e. it is defined in the infinite time limit, the above question can be addressed by analysing the behavior of the transverse Lyapunov exponent evaluated at finite times. In particular, suppose we distribute a large number of initial conditions in \mathcal{M} , compute $\Lambda_1^T(t)$ for each trajectory at time t , and then construct the histogram of these finite time exponents. Typically, the histogram is centered at Λ_1^T with a width that is proportional to $1/\sqrt{t}$. Thus, at any finite time, the distribution of $\Lambda_1^T(t)$ will have a tail on the negative side, indicating that some trajectories actually experience attraction towards \mathcal{M} . By the ergodicity of chaotic trajectories in \mathcal{M} , we see that a single trajectory, while in general repelled from \mathcal{M} , will experience episodes of time during which it is actually attracted towards \mathcal{M} . Thus, an observation is that the trajectory tends to stay near \mathcal{M} which bursts away from it at random times, signifying on-off intermittency. At the onset of on-off intermittency, i.e. when $\Lambda_1^T = 0$, the time interval between two successive bursts, or the *laminar phase*, obeys a power-law probability distribution with the exponent $-3/2$ (Heagy *et al.*, 1994).

The mechanism for chaotic synchronization and on-off intermittency can also be understood by analysing the transverse stabilities of the infinite set of unstable periodic orbits embedded in the chaotic attractor in \mathcal{M} (Nagai & Lai, 1997). The key observation is that the chaotic attractor in \mathcal{M} has embedded an infinite number of unstable periodic orbits within itself, and a transition from stable synchronization to on-off intermittency is caused by the change in the transverse stability of a *typical trajectory with respect to the natural measure* on the chaotic attractor in \mathcal{M} . Such a trajectory visits the neighborhoods of the infinite number of unstable periodic orbits from time to time. The periodic orbits embedded in the chaotic attractor are *atypical* in the sense that they form a Lebesgue measure zero set. With probability one, randomly chosen initial conditions do not yield trajectories which live on unstable periodic orbits. Invariant measures produced by unstable periodic orbits are thus atypical, and there are an infinite number of such atypical invariant measures embedded in a chaotic attractor. The natural measure, on the other hand, is typical in the sense that it is generated by

a trajectory originated from any one of the randomly chosen initial conditions in the basin of attraction. In this sense, chaos can be considered as being organized with respect to the unstable periodic orbits. In systems that exhibit synchronization, the transverse stability of a typical trajectory in \mathcal{M} is thus determined by the transverse stability of the infinite number of unstable periodic orbits which the trajectory visits in different time intervals. Among these periodic orbits, some are transversely stable and the others are transversely unstable near the bifurcation. If “more” periodic orbits are transversely stable (unstable), the typical trajectory is transversely stable (unstable). The transition occurs when there are approximately equal numbers of the transversely stable and unstable periodic orbits so that on average, the typical trajectory experiences exactly equal amount of attraction towards and repulsion away from the invariant subspace \mathcal{M} . Since there are an infinite number of periodic orbits in the chaotic attractor, the transition must then involve the change in the transverse stability of an infinite number of periodic orbits.

When the two-coupled maps are non-identical, i.e. $\mathbf{f}_1 \approx \mathbf{f}_2$, in the (\mathbf{u}, \mathbf{v}) coordinate, utilizing Taylor’s expansion to the first order in eqn (4) yields

$$\begin{aligned} \mathbf{u}_{n+1} &\approx \frac{1}{2} [\mathbf{f}_1(\mathbf{u}_n) + \mathbf{f}_2(\mathbf{u}_n)] + \frac{1}{2} \mathbf{J}_1(\mathbf{u}_n) - \mathbf{J}_2(\mathbf{u}_n) \cdot \mathbf{v}_n, \\ \mathbf{v}_{n+1} &\approx \frac{1}{2} [\mathbf{J}_1(\mathbf{u}_n) + \mathbf{J}_2(\mathbf{u}_n) - 4\mathbf{C}] \cdot \mathbf{v}_n \\ &\quad + \frac{1}{2} [\mathbf{f}_2(\mathbf{u}_n) - \mathbf{f}_1(\mathbf{u}_n)] \equiv \overline{\mathbf{J}(\mathbf{u}_n)} \cdot \mathbf{v}_n + \frac{1}{2} \Delta \mathbf{f}(\mathbf{u}_n), \end{aligned} \quad (13)$$

where the approximation $|\mathbf{v}| \ll |\mathbf{u}|$ is used. Thus, we see that the map for \mathbf{u} is approximately the average of \mathbf{f}_1 and \mathbf{f}_2 and, hence, we expect \mathbf{u} to be chaotic. The key point here is that the synchronization state (i.e. $\mathbf{v} = 0$) is no longer a solution of eqn (13) and, hence, the synchronization manifold \mathcal{M} is not an invariant manifold. As a result, the notion of transverse Lyapunov spectrum no longer holds. If the coupling is strong enough, a trajectory can still approach \mathcal{M} and stay in its vicinity, but this approximate synchronization state usually cannot be maintained indefinitely. In fact, the term $\frac{1}{2} [\mathbf{f}_2(\mathbf{u}_n) - \mathbf{f}_1(\mathbf{u}_n)]$ in

the \mathbf{v} equation in eqn (13) can be regarded as an additive random noise term, because \mathbf{u}_n is chaotic. This additive noise term can destroy the near synchronization state, leading to a burst away from it. Thus, we expect on-off intermittency to be more prevalent than that in the identical map case. We remark, however, that robust synchronization can still occur when the maps are non-identical, but very large coupling is required so that no finite-time Lyapunov exponent computed using $\bar{\mathbf{J}}$ can be positive. This demands, in terms of unstable periodic orbits embedded in the chaotic process \mathbf{u} , that no orbit has expanding eigenvalues in the \mathbf{v} subspace.

3.2. NONLINEARLY COUPLED MAPS

We now consider the more general case of a system of coupled maps with a *nonlinear* coupling scheme of the form

$$\begin{aligned}\mathbf{x}_{n+1} &= \mathbf{f}_1(\mathbf{x}_n) + \mathbf{C} \cdot [\mathbf{g}_1(\mathbf{y}_n) - \mathbf{f}_1(\mathbf{x}_n)], \\ \mathbf{y}_{n+1} &= \mathbf{f}_2(\mathbf{y}_n) + \mathbf{C} \cdot [\mathbf{g}_2(\mathbf{x}_n) - \mathbf{f}_2(\mathbf{y}_n)],\end{aligned}\quad (14)$$

where the variables are defined as in the linearly coupled case, eqn (4), and \mathbf{g}_1 and \mathbf{g}_2 are nonlinear functions. Equation (14) is more germane to the Holt–McPeek model [eqn (3)], which can be seen by making the following correspondence: $\mathbf{x}_n \leftrightarrow (N_{11}, N_{21})$, $\mathbf{y}_n \leftrightarrow (N_{12}, N_{22})$, $\mathbf{f}_1 \leftrightarrow \mathbf{W}_1(N_{11}, N_{21})$, $\mathbf{f}_2 \leftrightarrow \mathbf{W}_2(N_{12}, N_{22})$, $\mathbf{g}_1 \leftrightarrow m\mathbf{W}_2(N_{12}, N_{22})$, $\mathbf{g}_2 \leftrightarrow m\mathbf{W}_1(N_{11}, N_{21})$, and

$$\mathbf{C} \leftrightarrow \begin{pmatrix} e_1 & 0 \\ 0 & e_2 \end{pmatrix}.$$

In a qualitative sense, the Holt–McPeek model is thus contained in eqn (14).

We first consider the situation of identical maps: $\mathbf{f}_1 = \mathbf{f}_2 = \mathbf{f}$ and $\mathbf{g}_1 = \mathbf{g}_2 = \mathbf{g}$. Using the same approach as for linearly coupled maps, we find that the stability of the synchronization manifold \mathcal{M} is (in the $\{\mathbf{u}, \mathbf{v}\}$ coordinate frame)

$$\begin{aligned}\mathbf{u}_{n+1} &= (\mathbf{I} - \mathbf{C}) \cdot \mathbf{f}(\mathbf{u}_n) + \mathbf{C} \cdot \mathbf{g}(\mathbf{u}_n), \\ \mathbf{v}_{n+1} &= [\mathbf{J}_f(\mathbf{u}_n) - \mathbf{C} \cdot (\mathbf{J}_g(\mathbf{u}_n) + \mathbf{J}_f(\mathbf{u}_n))] \cdot \mathbf{v}_n,\end{aligned}\quad (15)$$

where \mathbf{I} is the identity matrix, $\mathbf{J}_f(\mathbf{u}_n)$ and $\mathbf{J}_g(\mathbf{u}_n)$ are the Jacobian matrices of the vector functions \mathbf{f} and \mathbf{g} , respectively, evaluated at $\mathbf{v}_n = \mathbf{0}$. As in the linearly coupled-identical-map case, we see that the \mathbf{u} dynamics provide random driving to the transverse subspace \mathcal{T} . In order for there to be an instability in \mathcal{T} , we see that the map $(\mathbf{I} - \mathbf{C}) \cdot \mathbf{f}(\mathbf{u}_n)$ must be chaotic, in contrast to the earlier case in eqn (10) where only $\mathbf{f}(\mathbf{u})$ needs to be chaotic. In this case, \mathbf{v} is unstable whenever \mathbf{u} is; therefore, \mathcal{T} becomes unstable as \mathcal{M} becomes chaotic. However, if $\mathbf{f} \approx \mathbf{g}$, then the dynamics of \mathbf{u} are governed by $\mathbf{f}(\mathbf{u}_n)$ with a small additive term generated by the coupling. In this situation, the onset of instability of the transverse subspace will no longer coincide with the onset of chaos inside manifold \mathcal{M} . Instead, there will be some critical value of the coupling constant where \mathcal{T} becomes unstable, as in the case of linearly coupled, identical maps.

For the case where the maps are not identical but only slightly different: $\mathbf{f}_1 \approx \mathbf{f}_2$ and $\mathbf{g}_1 \approx \mathbf{g}_2$, we obtain from eqn (14),

$$\begin{aligned}\mathbf{u}_{n+1} &\approx \frac{(1 - \mathbf{C})}{2} \cdot [\mathbf{f}_1(\mathbf{u}_n) + \mathbf{f}_2(\mathbf{u}_n) + (\mathbf{J}_{f_1}(\mathbf{u}_n) \\ &\quad + \mathbf{J}_{f_2}(\mathbf{u}_n)) \cdot \mathbf{v}_n] + \frac{\mathbf{C}}{2} \cdot [\mathbf{g}_1(\mathbf{u}_n) + \mathbf{g}_2(\mathbf{u}_n) \\ &\quad + (\mathbf{J}_{g_1}(\mathbf{u}_n) + \mathbf{J}_{g_2}(\mathbf{u}_n)) \cdot \mathbf{v}_n], \\ \mathbf{v}_{n+1} &\approx \frac{(1 - \mathbf{C})}{2} \cdot [\mathbf{f}_1(\mathbf{u}_n) - \mathbf{f}_2(\mathbf{u}_n) + (\mathbf{J}_{f_1}(\mathbf{u}_n) \\ &\quad + \mathbf{J}_{f_2}(\mathbf{u}_n)) \cdot \mathbf{v}_n] + \frac{\mathbf{C}}{2} \cdot [\mathbf{g}_1(\mathbf{u}_n) - \mathbf{g}_2(\mathbf{u}_n) \\ &\quad + (\mathbf{J}_{g_1}(\mathbf{u}_n) + \mathbf{J}_{g_2}(\mathbf{u}_n)) \cdot \mathbf{v}_n],\end{aligned}\quad (16)$$

where $\mathbf{J}_{f_1}(\mathbf{u}_n)$, $\mathbf{J}_{f_2}(\mathbf{u}_n)$, $\mathbf{J}_{g_1}(\mathbf{u}_n)$, and $\mathbf{J}_{g_2}(\mathbf{u}_n)$ are the Jacobian matrices of the vector functions \mathbf{f}_1 , \mathbf{f}_2 , \mathbf{g}_1 , and \mathbf{g}_2 , respectively, evaluated at $\mathbf{v}_n = \mathbf{0}$. Regarding the $\left(\frac{1}{2}(1 - \mathbf{C}) \cdot \{\mathbf{f}_1(\mathbf{u}_n) - \mathbf{f}_2(\mathbf{u}_n) + \mathbf{C} \cdot [\mathbf{g}_1(\mathbf{u}_n) - \mathbf{g}_2(\mathbf{u}_n)]\}\right)$ term as an additive random noise term due to \mathbf{u}_n being chaotic, we obtain a similar result as for the linearly coupled case, i.e. on-off intermittency can be common.

4. Numerical Results with the Holt–McPeek Model

4.1. SYNCHRONIZATION AND ON-OFF INTERMITTENCY

Regarding the two patches in the Holt–McPeek model equation (3) as two coupled systems, we examine the total populations in both patches: $N_{t1} = N_{11} + N_{21}$ and $N_{t2} = N_{12} + N_{22}$. Figure 5 plots N_{t1} vs. N_{t2} for a trajectory of 10^4 points (after discarding an initial transient of 10^3 iterations). We observe that the trajectory points tend to lie in the vicinity of the line defined by \mathcal{L} : $N_{t1}/K_1 = N_{t2}/K_2$, with occasional deviations away from it. The line \mathcal{L} is thus the synchronization manifold of eqn (3) in a general sense, as there is no direct (one-to-one) synchronization between the corresponding dynamical variables in the two patches. Such “indirect” synchronization is also called *generalized synchronization* (Abarbanel *et al.*, 1995). The time trace $Q(t)$ [eqn (1)] exhibits an intermittent behavior, as shown in Fig. 6(a). We see that most of the time, Q remains close to zero, signifying synchronization. However, the synchronization state is interspersed with occasional bursts away from it. Figure 6(a) shows a typical on-off intermittency. The laminar-phase distribution of the time series in Fig. 6(a) appears to exhibit an approximate power-law scaling with an exponential tail,

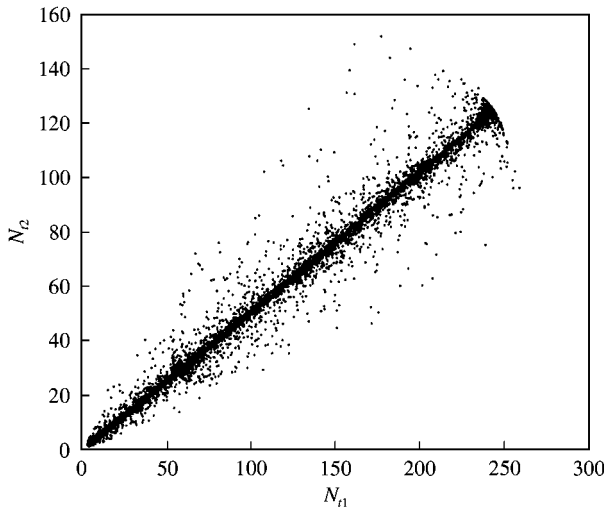


FIG. 5. Total population of patch 2 ($N_{t2} = N_{12} + N_{22}$) vs. total population of patch 1 ($N_{t1} = N_{11} + N_{21}$). Parameters are set at the same values as in Fig. 3.

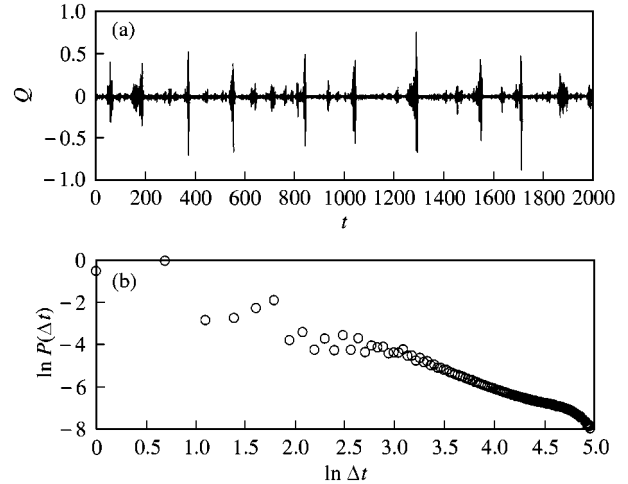


FIG. 6. For the parameters in Fig. 2 and after discarding 10^3 iterates. (a) Q vs. iterate and (b) a histogram of the distribution of time intervals between $Q > Q_{\min}$.

as shown in Fig. 6(b). To obtain Fig. 6(b), a threshold $Q_{th} = 0.01$ (arbitrary) is set and time intervals Δt in which $Q(t)$ falls below Q_{th} are accumulated to yield a histogram. We observe that in the range of approximate power-law behavior, the slope of the distribution is about -1.3 . Since the system is non-identical, a transverse Lyapunov exponent cannot be defined, thus it may not be reasonable to expect that the slope would be precisely the same as was found at the onset of on-off intermittency in an identical case. [Strictly speaking, the -1.5 algebraic exponent in the distribution of laminar phases occurs only at the onset of the on-off intermittency (Heagy *et al.*, 1994). In parameter regimes away from the onset, the algebraic behavior only occurs at small intervals of Δt with no universal exponent. The laminar-phase distribution is typically exponential for large values of Δt . These are in fact observed in our numerical experiments.]

Of importance to the problem of coexistence is the parameter m , the fraction of the dispersing population that can compete with the resident population [($1 - m$) is the cost of dispersal]. If m is too small, or the cost of dispersal is too high, then generally the dispersing species will be extinct. In numerical experiments we find that, insofar as chaos is present, the minimum values of m for coexistence can be as low as 0.3. Figure 7(a) and (b) shows, for $m = 0.8$, the apparent on-off

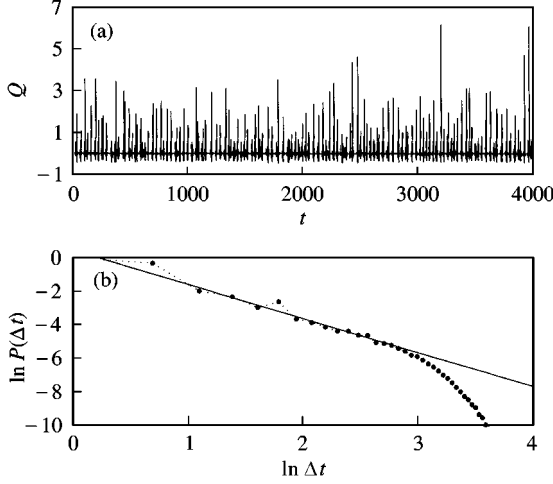


FIG. 7. For $m = 0.8$ in the Holt-McPeek model equation (3): (a) On-off intermittency in $Q(t)$, quality of synchronization; (b) a histrogram of the distribution of the laminar phase.

intermittent behavior in $Q(t)$ and the distribution of the corresponding laminar phases, respectively. There is still a range of Δt in which the distribution appears algebraic, followed by an exponential tail. The algebraic exponent is approximately -2 .

4.2. COUPLING MECHANISM IN THE HOLT-MCPEEK MODEL

To better understand how synchronization and on-off intermittency occur in coupled ecological models such as eqn (3), it is necessary to understand and characterize the coupling mechanism. For coupled systems such as eqn (4), coupling is defined by the matrix \mathbf{C} in a straightforward manner. The Holt-McPeek model equation (3), however, cannot be reduced to the form of eqn (4). Instead, each term in the model equations contains nonlinear coupling through the fitness, W_j , and the model can be reduced to the form of eqn (14). From an ecological perspective, the coupling consists of the movement of organisms between patches, which is affected both by the relative fitness in the patches and the average dispersal rate of the population. If the instantaneous average dispersal rate of the population is high, then there is a lot of spatial movement and the effective coupling between the patches is high. However, if the opposite is true and the

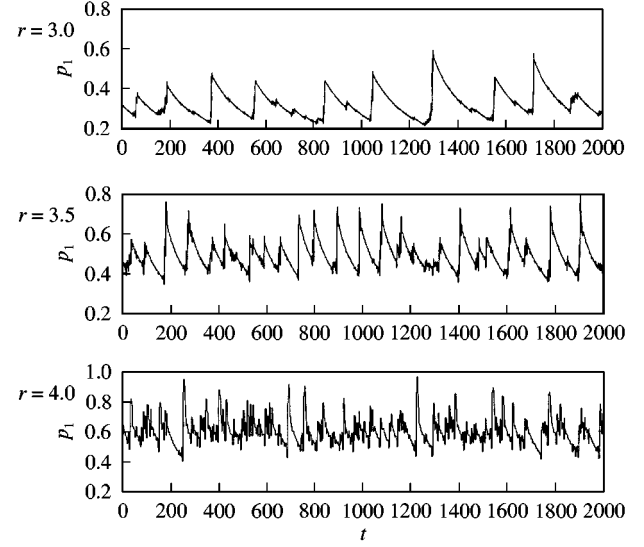


FIG. 8. Time series for the Holt-McPeek model at various values of r and $e_1 = 0.5$, $e_2 = 0.01$, $K_1 = 100$, $K_2 = 50$, and $m = 1$. We observe that the spacing between kicks in p_1 decreases as r is increased.

average dispersal rate of the population is low, then the population is more sedentary and the effective coupling between the two patches is smaller. Since the two species in our model have greatly disparate dispersal rates, a convenient way of examining the average dispersal behavior of the system is to look at the frequency of the high-dispersal clone, p_1 . Obviously, as p_1 increases, so will the average dispersal rate of the entire population at a given time.

So, we now consider how the behavior of p_1 changes as the growth rate r is varied. Figure 8 shows the time trace $p_1(t)$ at different r values. We observe that, as r is increased, the jumps in $p_1(t)$ become more often and overall, $p_1(t)$ increases. Figure 9 shows \bar{p}_1 , the average value of p_1 , vs. r , where we see that \bar{p}_1 increases fairly steadily. As the intrinsic growth rate increases, the high-dispersal clone becomes more prevalent and we expect to see more movement between the two patches. The effective coupling between the two patches then increases with r .

The parameter r , however, also controls how chaotic the patch dynamics can become. To see this, we compute the convergence or divergence of nearby trajectories through the Lyapunov spectrum using the standard procedure by Benettin *et al.* (1980). Figure 10 shows the first three

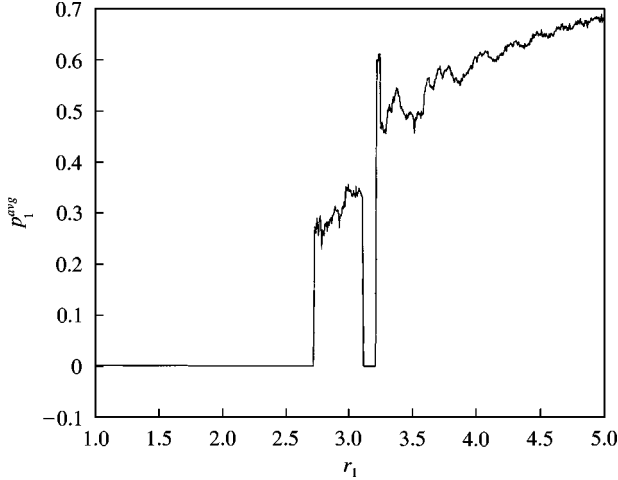


FIG. 9. Average frequency of the high-dispersal clone vs. the growth rate r . Parameters set as in Fig. 2.

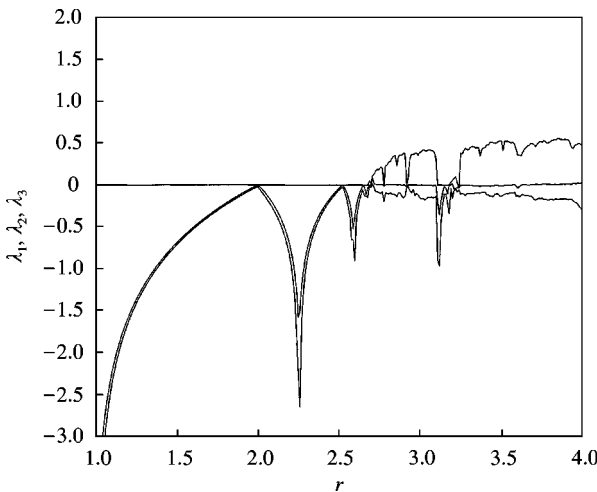


FIG. 10. The first three Lyapunov exponents of the model vs. the parameter r . The other parameters are set as in Fig. 11.

Lyapunov exponents vs. r , where we see that the magnitude of the largest one increases as r is increased (except when there are periodic windows), indicating that the patch dynamics become more chaotic. We also see that, for $r < 2.7$, there are two negative Lyapunov exponents and one at zero. The fourth Lyapunov exponent (not shown) is strongly negative throughout the entire range of the plot. After the transition to chaos, the first positive Lyapunov exponent tends to increase (except when in periodic windows).

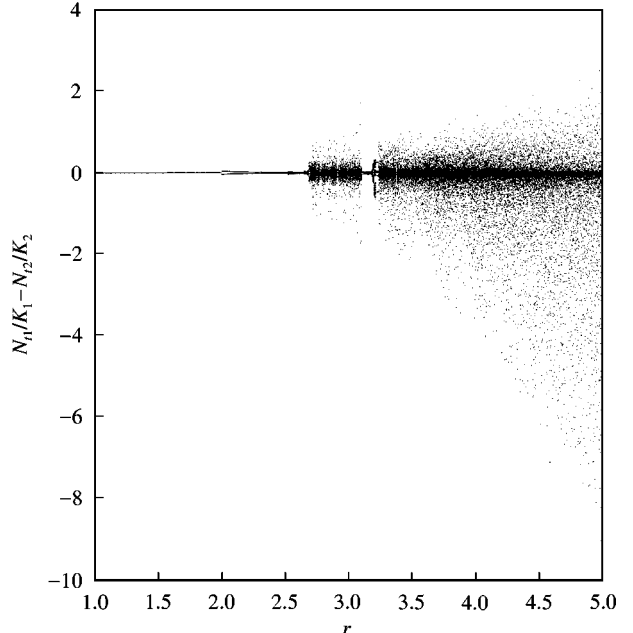


FIG. 11. Bifurcation diagram of $N_{t1}/K_1 - N_{t2}/K_2$ for the Holt-McPeek model with $e_1 = 0.5$, $e_2 = 0.01$, $K_1 = 100$, $K_2 = 50$, and $m = 1$.

As r is increased above the critical point for chaos, two competing factors emerge: the system becomes more chaotic, but the coupling between the two patches becomes stronger. Consequently, for large r values, we expect to see a more robust synchronization state, corresponding to small variations in the Q value in the synchronization state, but the range of the bursts from the $Q \approx 0$ state increases as well, as shown in Fig. 11. In particular, this bifurcation diagram is constructed by iterating the system from a random initial condition 10^3 times after discarding an initial 10^4 iterates for a given parameter r . The value of r is then incremented through a small step size of 10^{-3} , and the process is repeated with a new random initial condition. We see that the system is in the vicinity of the generalized synchronization manifold \mathcal{L} until r is approximately 2.7, after which chaos and on-off intermittency arises. Here, there is a high concentration of trajectory points near \mathcal{L} , indicating that the system tends to stay in the vicinity of the synchronization state. However, there are short-time periods during which the trajectory bursts away from \mathcal{L} . As r increases further, trajectory points tend to concentrate more closely near \mathcal{L} , indicating the

effect of a stronger coupling. However, the range of bursts also increases as the system becomes “more” chaotic.

4.3. REMARKS

1. The relatively rapid rise and slow decline in the time evolution of the frequency $p_1(t)$ of the high-dispersal clone, as shown in Fig. 2, can be understood, as follows. As $p_1(t)$ decreases and becomes small, the coupling between the dynamics in different patches is weakened because of the decrease in the dispersing population. When the coupling becomes sufficiently weak, de-synchronization between the patch dynamics occurs, which corresponds to the “on” state in $Q(t)$. It is known that in on-off intermittency, the “on” state, or the burst, occurs in time intervals that are typically much shorter than those for the “off” state (Spiegel, 1980; Fujisaka & Yamada, 1985, 1986; Fujisaka *et al.*, 1986; Yu *et al.*, 1991; Platt *et al.*, 1993; Heagy *et al.*, 1994; Lai & Grebogi, 1995; Lai, 1996a, b; Yalcinkaya & Lai, 1996; Venkataramani *et al.*, 1995, 1996; Marthaler *et al.*, 2001), because dynamically bursting occurs when the trajectory is sufficiently near a transversely unstable set, such as a transversely unstable periodic orbit, and is therefore exponentially fast (in contrast, the “off” state corresponds to the trajectory’s wandering through many transversely stable sets, which tends to keep the trajectory in the “off” state for a long time). The key point is that a de-synchronization state therefore generates a high degree of temporal variation, which favors dispersal and causes a rapid growth of the dispersing population. This, in turn, tends to synchronize population dynamics in the two patches. The synchronization state corresponds to the “off” state in $Q(t)$, which can typically be maintained for a relatively long time. As synchronization tends to disfavor dispersal, during the “off” state the frequency of the high-dispersal clone declines, the patch dynamics then become progressively uncoupled, and the whole process repeats itself over and over again in the course of time evolution.

2. As the dispersal rate is increased so that the coupling becomes stronger, the chaotic synchronization state becomes more robust. The theoretical analysis in Section 3 indicates that perfect

synchronization, i.e. synchronization without on-off intermittency, would have been realized if the system had a perfect invariant subspace. Such a perfect synchronization would lead to coexistence as well, because there is still chaos and therefore the required temporal variation. The Holt–McPeek model, nonetheless, does not possess a perfect invariant subspace. Synchronization in the model is thus always intermittent. As we shall discuss in Appendix A, for a class of simplified models derived from the Holt–McPeek model, a perfect invariant subspace can possibly exist, which in turn, leads to coexistence under perfect chaotic synchronization (see, for example, Fig. A3).

5. Discussion

Understanding the factors generating and maintaining the species diversity of ecological communities is one of the central goals of the ecological sciences. In the last several decades, ecologists have become increasingly aware of the importance of processes operating at large temporal and spatial scales in explaining patterns of species diversity in local communities (Rosenzweig, 1995). This is particularly the case when considering guilds of organisms utilizing limited resources in similar ways. In spatially closed, homogeneous systems which dynamically settle into a point equilibrium, species sharing limited resources often show competitive exclusion. Since any given spatial location has a limited variety and quantity of resources, competition is a local process which tends to limit local species diversity. This local process in nature, however, interacts with other processes. For instance, if local dynamics do not achieve a point equilibrium (e.g. limit-cycle behavior in multispecies resource-consumer interactions (Armstrong & McGehee, 1980), consumer species can share resources yet still coexist. Many ecologists contend that patterns in species diversity cannot be understood without reference to nonequilibrium dynamics (Huston, 1994). Indeed, many ecologists now believe that “space is the final frontier” for addressing classical ecological problems (Kareiva, 1994; Ricklefs & Schlüter, 1993).

The fundamental dynamics in spatially extended ecological systems relies on dispersal,

which provides the interaction among species in the spatially extended environment. It is thus of paramount importance to understand under what conditions dispersal favors species coexistence. It has been shown (Hastings, 1983; Holt, 1985) that spatial heterogeneity in abundance alone is unable to select for dispersal. To favor dispersal, some temporal heterogeneity must also be present. Many previous theoretical treatments (for example, Gadgil, 1971; Balkau & Feldman, 1973; Roff, 1975; Asmussen, 1983; Metz *et al.*, 1983) have assumed that external environmental variation supplies the required driving force to create temporal variation in fitness. However, in view of the ubiquity of nonlinearity in ecological systems, it is reasonable that nonlinear population dynamics leading to cycles or chaotic behaviors can produce the appropriate temporal variation in fitness that favors the evolution of dispersal. This has been suggested both theoretically (Holt & McPeek, 1996; Doebeli & Ruxton, 1997; Parvinen, 1999) and empirically (e.g. Kendall *et al.*, 1998).

The main contributions to our work are two-fold: (1) we provide analysis and evidence that chaotic dynamics in spatially coupled ecological models can indeed provide the spatiotemporal variation in fitness that is necessary for the coexistence of dispersing species; and (2) we show that under fairly general settings, the spatiotemporal variation in fitness leads to on-off intermittency, with respect to the approximate synchronization of the relative patch populations. As such, it is likely that synchronization and on-off intermittency can be a contributing dynamical factor for the coexistence of species in ecological systems.

Another important issue in ecology is the possibility of long transient behavior in population dynamics. An important contribution along this line is made by Hastings & Higgins (1994), who report their finding of very long transient behaviors in spatially extended ecological models for a species with alternating reproduction and dispersal. They demonstrate, through numerical computations, that if the nonlinearity in the model is strong enough, then the time required to reach the asymptotic dynamics can approach thousands of generations—a time that is much longer than the time scale of significant

environmental perturbations and therefore can be considered extremely long on ecological time-scales of the species where the typical time-scale of interest in tens or hundreds of years. Since the form of dynamics changes over long time-scales, it is argued that transient dynamics of ecological models may be more relevant than long-term behavior (Hastings & Higgins, 1994). This conclusion is quite surprising for the field of quantitative ecology because traditionally, ecological theory has been based on long-term behavior of ecological models, with stability analysis of the asymptotic state as the primary tool (May, 1973; Roughgarden *et al.*, 1989; Hastings, 1993). The occurrence of on-off intermittency in spatially extended ecological systems indicates, however, that the nearly synchronous chaotic dynamics in these systems is sustained, as is evident from the dynamical mechanism that leads to on-off intermittency that we have described in this work. It is an interesting problem, for future work, to examine how often one can actually expect transient or sustained chaotic dynamics in ecological systems.

This work was supported by NSF under Grant no. DMS-9626529. YCL was also supported by NSF under Grant no. PHY-9996454, and RDH was supported by NSF DEB-9528602.

REFERENCES

- ABARBANEL, H. D. I., RULKOV, N. F. & SUSHCHIK, M. (1996). Generalized synchronization of chaos: the auxiliary system approach. *Phys. Rev. E* **53**, 4528–4535.
- ARMSTRONG, R. A. & McGHEE, R. (1980). Competitive exclusion. *Am. Nat.* **115**, 151–170.
- ASMUSSEN, M. A. (1983). Evolution of dispersal in density-regulated populations: a haploid model. *Theor. Pop. Biol.* **23**, 281–299.
- BALKAU, M. J. & FELDMAN, M. W. (1973). Selection for migration modification. *Genetics* **74**, 171–174.
- BARRETO, E., SO, P., GLUCKMAN, B. J. & SCHIFF, S. J. (2000). From generalized synchrony to topological decoherence: emergent sets in coupled chaotic systems. *Phys. Rev. Lett.* **84**, 1689–1692.
- BENETTIN, G., GALGANI, L., GIORGILLI, A. & STREL'CYN, J.-M. (1980). Lyapunov characteristic exponents for smooth dynamical systems and for Hamiltonian systems. a method for computing all of them. Part 2: numerical application. *Mecanica* **15**, 9–30.
- CHESSON, P. L. (1986). Environmental variation and the coexistence of species. In: *Community Ecology* (Diamond, J. & Case T. J., eds), pp. 240–256. New York: Harper & Row.
- COHEN, D. & LEVIN, S. A. (1991). Dispersal in patchy environments — the effects of temporal and spatial structure. *Theor. Popul. Biol.* **39**, 63–99.

- COMINS, H. N. (1982). Evolutionary stable strategies for localized dispersal in 2 dimensions. *J. theor. Biol.* **94**, 579–606.
- DOEBELI, M. & RUXTON, G. D. (1997). Evolution of dispersal rates in metapopulation models—branching and cyclic dynamics in phenotype space. *Evolution* **51**, 1730–1741.
- FERRIERE, R. & CAZELLES, B. (1999). Universal power laws govern intermittent rarity in communities of interacting species. *Ecology* **80**, 1505–1521.
- FUJISAKA, H. & YAMADA, T. (1985). A new intermittency in coupled dynamical systems. *Prog. Theor. Phys.* **74**, 918–921.
- FUJISAKA, H. & YAMADA, T. (1986). Stability theory of synchronized motion in coupled-oscillator systems: 4. Instability of synchronized chaos and new intermittency. *Prog. Theor. Phys.* **75**, 1087–1104.
- FUJISAKA, H., ISHII, H., INOUE, M. & YAMADA, T. (1986). Intermittency caused by chaotic modulation: 2. Lyapunov exponent, fractal structure, and power spectrum. *Prog. Theor. Phys.* **76**, 1198–1209.
- GADGIL, M. (1971). Dispersal-population consequences and evolution. *Ecology* **52**, 253–261.
- GROVER, J. P. (1997). *Resource Competition*. London: Chapman & Hall.
- HAMILTON, W. D. & MAY, R. M. (1977). Dispersal in stable habitats. *Nature (London)* **269**, 578–581.
- HANSKI, I. (1999). *Metapopulation Ecology*. Oxford: Oxford University Press.
- HASTINGS, A. (1983). Can spatial variation alone lead to selection for dispersal? *Theor. Popul. Biol.* **24**, 244–251.
- HASTINGS, A. & HIGGINS, K. (1994). Persistence of transients in spatially structured ecological models. *Science* **263**, 1133–1136.
- HASTINGS, A., HOM, C. L., ELLNER, S., TURCHIN, P. & GODFRAY, H. C. J. (1993). Chaos in ecology—is mother nature a strange attractor? *Ann. Rev. Ecol. Systemat.* **24**, 1–33.
- HEAGY, J. F., PLATT, N. & HAMMEL, S. M. (1994). Characterization of on-off intermittency. *Phys. Rev. E* **49**, 1140–1150.
- HOLT, R. D. (1985). Population dynamics in 2-patch environments—some anomalous consequences of an optimal habitat distribution. *Theor. Popul. Biol.* **28**, 181–208.
- HOLT, R. D. & MCPEEK, M. A. (1996). Chaotic population-dynamics favors the evolution of dispersal. *Am. Nat.* **148**, 709–718.
- HOLT, R. D., GROVER, J. & TILMAN, D. (1994). Simple rules for interspecific dominance in systems with exploitative and apparent competition. *Am. Nat.* **144**, 741–771.
- HUSTON, M. (1994). *Biological Diversity: The Coexistence of Species on Changing Landscapes*. Cambridge: Cambridge University Press.
- HUTCHINSON, G. E. (1978). *An Introduction to Population Ecology*. New Haven, CT: Yale University Press.
- KAPLAN, D. T. (1994). Exceptional events as evidence for determinism. *Physica D* **73**, 38–48.
- KENDALL, B. E., PRENDERGAST, J. & BJØRNSTAD, O. N. (1998). The macroecology of population dynamics: taxonomic and biogeographic patterns in population cycles. *Ecol. Lett.* **1**, 160–164.
- KAREIVA, P. (ed.) (1994). Space: The Final Frontier for Ecological Theory, *Ecology* **75**, 1–47.
- KUNO, E. (1981). Dispersal and the persistence of populations in unstable habitats—a theoretical note. *Oecologia (Berlin)* **49**, 123–126.
- LAI, Y.-C. (1996a). Symmetry-breaking bifurcation with on-off intermittency in chaotic dynamical systems. *Phys. Rev. E* **53**, R4267–R4270.
- LAI, Y.-C. (1996b). Distinct small-distance scaling behavior of on-off intermittency in chaotic dynamical systems. *Phys. Rev. E* **54**, 321–327.
- LAI, Y.-C. & GREBOGI, C. (1995). Intermingled basins and two-state on-off intermittency. *Phys. Rev. E* **52**, R3313–R3316.
- LAW, R. (1999). Theoretical aspects of community ecology. In: *Advanced Ecological Theory* (McGlade, J., ed.), pp. 143–171. Oxford: Blackwell Science.
- LEHMAN, C. L. & TILMAN, D. (1997). Competition in spatial habitats. In: *Spatial Ecology: The Role of Space in Population Dynamics and Interspecific Interactions* (Tilman, D. & Kareiva, P., eds), pp. 185–203. Princeton, NJ: Princeton University Press.
- LEVIN, S. A., COHEN, D. & HASTINGS, A. (1984). Dispersal strategies in patchy environments. *Theor. Popul. Biol.* **26**, 165–191.
- LIBERMAN, U. & FELDMAN, M. W. (1989). The reduction principle for genetic modifiers of the migration rate, In: *Mathematical Evolutionary Theory* (Feldman, M. W., ed), pp. 111–137. Princeton, NJ: Princeton University Press.
- MARTHALER, D., ARMBRUSTER, D., LAI, Y.-C. & KOSTELICH, E. J. (2001). Perturbed on-off intermittency. *Phys. Rev. E* **64**, 016220(1–9).
- MAY, R. M. (1973). *Stability and Complexity in Model Ecosystems*. Princeton, NJ: Princeton University Press.
- MAY, R. M. & OSTER, G. F. (1976). Bifurcations and dynamic complexity in simple ecological models. *Am. Nat.* **110**, 573–599.
- METZ, J. A. J., DEJONG, T. J. & KLINKHAM, P. G. (1983). What are the advantages of dispersing—a paper by Kuno explained and extended. *Oecologia (Berlin)* **57**, 166–169.
- NAGAI, Y. & LAI, Y.-C. (1997). Periodic-orbit theory of the blowout bifurcation. *Phys. Rev. E* **56**, 4031–4041.
- OLIVIERI, I., MICHALAKIS, Y. & GOYON, P. H. (1995). Metapopulation genetics and the evolution of dispersal. *Am. Nat.* **146**, 202–228.
- PARVINEN, J. (1999). Evolution of migration in a metapopulation. *Bull. Math. Biol.* **61**, 531–550.
- PECORA, L. M. & CARROLL, T. L. (1998). Master stability functions for synchronized coupled systems. *Phys. Rev. Lett.* **80**, 2109–2112.
- PLATT, N., SPIEGEL, E. A. & TRESSER, C. (1993). On-off intermittency: a mechanism for bursting. *Phys. Rev. Lett.* **70**, 279–282.
- RICKLEFS, R. & SCHLUTER, D. (1993). *Species Diversity in Ecological Communities*. Chicago: University of Chicago Press.
- ROFF, D. A. (1975). Population stability and evolution of dispersal in a heterogeneous environment. *Oecologia (Berlin)* **19**, 217–237.
- ROSENZWEIG, M. (1995). *Species Diversity in Space and Time*. Cambridge, NY: Cambridge University Press.
- ROUGHGARDEN, J. & DIAMOND, J. (1986). Overview: the role of species interactions in community ecology. In: *Community Ecology* (Diamond, J. & Case, T. J., eds), pp. 333–343. New York: Harper & Row.
- ROUGHGARDEN, J., MAY, R. M. & LEVIN, S. A. (1989). *Perspectives in Ecological Theory*. Princeton, NJ: Princeton University Press.

- SPIEGEL, E. A. (1980). A class of ordinary differential equations with strange attractors. *Ann. NY Acad. Sci.* **357**, 305–312.
- STONE, L., LANDAN, G. & MAY, R. M. (1996). Detecting time's arrow: a method for identifying nonlinearity and deterministic chaos in time-series data. *Proc. Roy. Soc. Lond. Ser. B* **263**, 1509–1513.
- SUGIHARA, G. & MAY, R. M. (1990). Nonlinear forecasting as a way to distinguish chaos from measurement error in time series. *Nature* **344**, 734–742.
- TAYLOR, P. D. (1988). An inclusive fitness model for dispersal of offspring. *J. theor. Biol.* **130**, 363–378.
- TOKESHI, M. (1999). *Species Coexistence: Ecological and Evolutionary Perspectives*. Oxford: Blackwell Science.
- VENKATARAMANI, S. C., ANTONSEN, T. M., OTT, E. & SOMMERER, J. C. (1995). Characterization of on-off intermittent time-series. *Phys. Lett. A* **207**, 173–179.
- VENKATARAMANI, S. C., ANTONSEN, T. M., OTT, E. & SOMMERER, J. C. (1996). On-off intermittency—power spectrum and fractal properties of time-series. *Physica D* **96**, 66–99.
- WIENER, P. & FELDMAN, M. W. (1991). The evolution of dispersal in a model of mixed selfing and random mating. *Evolution* **45**, 1717–1726.
- YALCINKAYA, T. & LAI, Y.-C. (1996). Blowout bifurcation route to strange nonchaotic attractors. *Phys. Rev. Lett.* **77**, 5039–5042.
- YU, L., OTT, E. & CHEN, Q. (1991). Fractal distribution of floaters on a fluid surface and the transition to chaos for random maps. *Physica D* **53**, 102–124.

APPENDIX A

One-clone Models

While numerical computations reveal that the Holt–McPeek model exhibits synchronization and on-off intermittency, it is difficult to reduce the model, say by changes of variables, mathematically to a form that is similar to one of the models treated in Section 3, for which the dynamical origin of synchronization and intermittency can be seen explicitly. We thus seek to construct simple models that are more amenable to analysis, while retaining the essential ecological ingredients of the Holt–McPeek model. The purpose of this appendix is to demonstrate that such a model can indeed be constructed, for which the combination of mathematical analysis and numerical computations gives a clear picture of the dynamics of chaotic synchronization and on-off intermittency.

The typical setting in addressing the coexistence problem in species dispersal, as in the Holt–McPeek model, is that one species is nearly stationary and another one is rapidly moving between patches. Coexistence is indicated by

a non-zero average population of the dispersing species. The influential dynamical variables are thus the populations of the dispersing species in different patches. As a reasonable approximation, we can regard the populations of the nearly stationary species as entirely stationary and drop these populations from consideration. The physical effects of the stationary populations, however, cannot be neglected. A reasonable assumption is that the stationary species only affects the resources available to the dispersing species but not contributing to dispersal itself. Accordingly, we consider a non-species, two-patch model where the existence of the stationary species (with its time-varying population densities) affects the system by imposing time-dependent resources availability. Consequently, the influence of the stationary clone is modeled in the system by the choice of $K_j(t)$'s, time-varying carrying capacities. The model then becomes

$$\begin{aligned} N_1(t+1) &= (1-e)W_1(t)N_1(t) + meW_2(t)N_2(t), \\ N_2(t+1) &= (1-e)W_2(t)N_2(t) + meW_1(t)N_1(t), \end{aligned} \quad (\text{A.1})$$

where the growth dynamics in the two patches are given by

$$W_1(t) = e^{r[1 - N_1(t)/K_1(t)]}, \quad W_2(t) = e^{r[1 - N_2(t)/K_2(t)]}. \quad (\text{A.2})$$

A.1. IDENTICAL PATCHES

When the patches are identical and the influence of the stationary clone is also identical, we have $K_1(t) = K_2(t) = K(t)$, and $r_1 = r_2 = r$. It is convenient to normalize the populations in terms of the carrying capacities and make the following change of variables:

$$\begin{aligned} u(t) &= \frac{1}{2} \left[\frac{N_1(t)}{K_1(t)} + \frac{N_2(t)}{K_2(t)} \right] \quad \text{and} \\ v(t) &= \frac{1}{2} \left[\frac{N_1(t)}{K_1(t)} - \frac{N_2(t)}{K_2(t)} \right]. \end{aligned}$$

or

$$\frac{N_1(t)}{K_1(t)} = u(t) + v(t) \quad \text{and} \quad \frac{N_2(t)}{K_2(t)} = u(t) - v(t).$$

In the new variables, we have

$$\begin{aligned} u(t+1) &= [AW_1(t) + AW_2(t)]u(t) \\ &\quad + [AW_1(t) - AW_2(t)]v(t), \\ v(t+1) &= [BW_1(t) - BW_2(t)]u(t) \\ &\quad + [BW_1(t) + BW_2(t)]v(t), \end{aligned} \quad (\text{A.3})$$

where $A = 1 - e + me$ and $B = 1 - e - me$. In the vicinity of the synchronization state, we have $v \approx 0$. We can use the Taylor expansion to the first order to obtain

$$e^{\pm rv(t)} \approx 1 \pm rv(t).$$

The time-dependent growth factors $W_{1,2}(t)$ thus become

$$\begin{aligned} W_1(t) &= e^{r[1-u(t)-v(t)]} \approx e^{r(1-u(t))} [1 - rv(t)], \\ W_2(t) &= e^{r[1-u(t)-v(t)]} \approx e^{r(1-u(t))} [1 + rv(t)]. \end{aligned} \quad (\text{A.4})$$

Near the synchronization state, $v(t) \approx 0$. Thus, to first order in v , we obtain (again by using Taylor expansions)

$$\begin{aligned} u(t+1) &= Ae^{[r(1-u(t))]} u(t), \\ v(t+1) &= Be^{[r(1-u(t))]} [1 - ru(t)]v(t). \end{aligned} \quad (\text{A.5})$$

A remarkable observation is that eqn (A.5) is similar to eqn (15), the model equation for synchronization and on-off intermittency in nonlinearly coupled, identical maps. This allows us to understand these dynamical phenomena in a more explicit way. For instance, we see that the synchronization state $v = 0$ is invariant under eqn (A.5) and, hence, if it is transversely stable, perfect synchronization $v = 0$ can be realized. The transverse Lyapunov exponent is given by

$$\begin{aligned} \Lambda^T &= \lim_{L \rightarrow \infty} \frac{1}{L} \sum_{t=0}^{L-1} B e^{[r(1-u(t))]} [1 - ru(t)] \\ &= \int B e^{[r(1-u)]} (1 - ru) \rho(u) du, \end{aligned} \quad (\text{A.6})$$

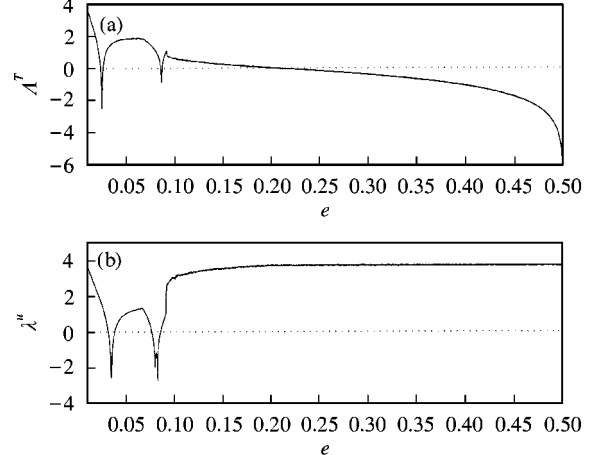


FIG. A1. For the one-clone, two identical patch model equation (19): (a) the transverse Lyapunov exponent Λ^T vs. the dispersal rate e , and (b) the Lyapunov exponent of the driving system u vs. e . Other parameters are $K = \text{ran}[100, 110]$ (a random parameter uniformly distributed between 100 and 110), $r = 4.0$, and $m = 1$.

where the summation over time is converted into an integral in space because of the ergodicity of chaos: a typical trajectory visits almost every part of the attractor in the course of time evolution, and $\rho(u)$ is the invariant density of the chaotic driving variable u . Figure A1(a) and (b) shows, respectively, the transverse Lyapunov exponent Λ^T and the Lyapunov exponent λ_u of the driving system u vs. the dispersal rate e of the clone for $r = 4.0$, $m = 1$, and $K(t) = \text{ran}[100, 110]$ (chosen randomly with uniform distribution between 100 and 110 at each iteration). We see that in the parameter regime where u is chaotic, Λ^T is negative for $e > e_c \approx 0.2$ and it is positive for $e \lesssim e_c$. Thus, we expect to observe perfect synchronization [i.e. $v(t \rightarrow \infty) \rightarrow 0$] for $e > e_c$. On-off intermittency occurs for $e \lesssim e_c$, as shown in Fig. A2 for $e = 0.19$. Figure A3(a-c) shows the bifurcation diagrams of N_1/K_1 , N_2/K_2 , and Q vs. e , respectively, where the range of synchronization and on-off intermittency can be seen.

To assess how synchronization and the on-off intermittent dynamics depend on the growth parameter r , we fix $e = 0.19$ and compute Q as a function of r , as shown in Fig. A4. We see regimes of perfect synchronization ($Q = 0$) interspersed with parameter intervals of on-off intermittent synchronization, which is characterized

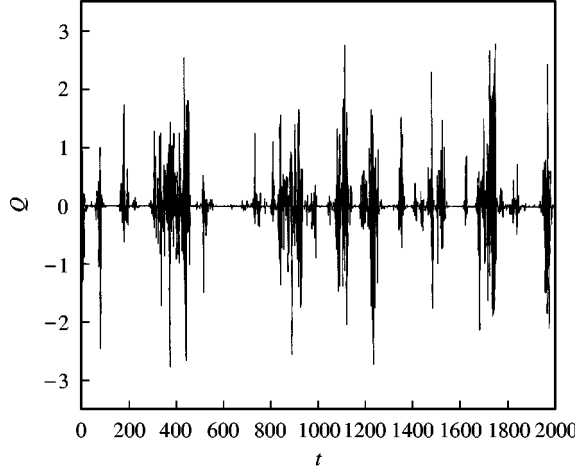


FIG. A2. For the one-clone, two identical patch model equation (19), on-off intermittency for $e = 0.19 < e_c$. Other parameters are the same as those in Fig. A1.

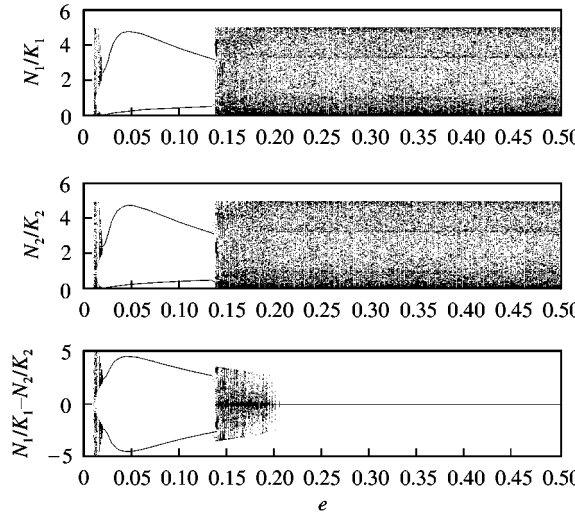


FIG. A3. Bifurcation diagrams for the one-clone, two identical patch model.

by non-zero values of Q , but a high concentration of Q near zero. Dynamically, on-off intermittency is due to the transverse Lyapunov exponent's being slightly positive, as shown in Fig. A5, where there is a correspondence between the parameter regimes for on-off intermittency in Fig. A4 and those in which Λ^T is slightly positive in Fig. A5.

A.2. NON-IDENTICAL PATCHES

When $K_1(t) \neq K_2(t)$, we obtain from eqn (A.1), in the (u, v) -coordinate, the following (still by

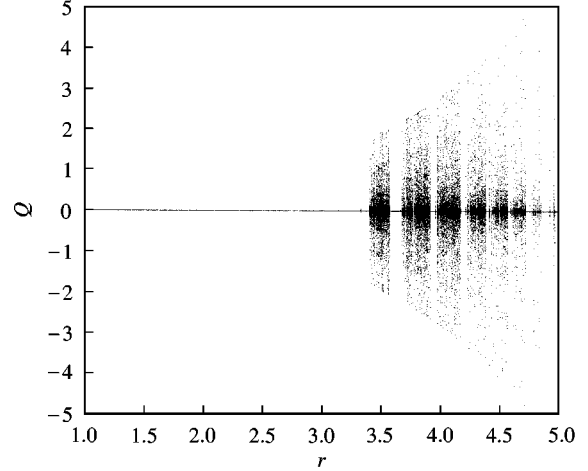


FIG. A4. For the one-clone, two identical patch model equation (19), the bifurcation diagram of Q vs. r .

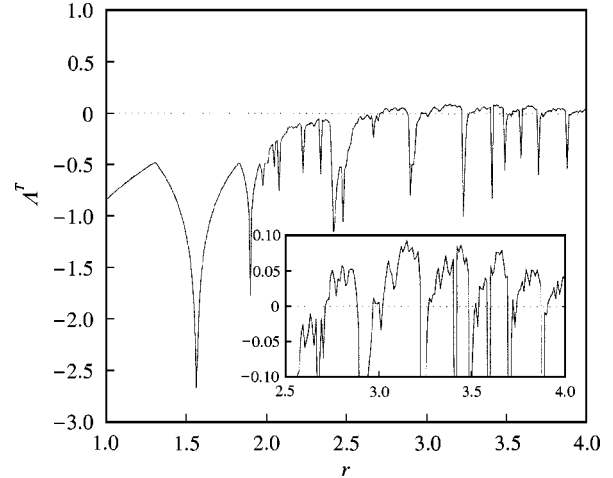


FIG. A5. For the one-clone, two identical patch model equation (19), the transverse Lyapunov exponent vs. r .

Taylor expansion to the first order in $v(t)$):

$$\begin{aligned} u(t+1) = & e^{r(1-u(t))} [A_+ u(t) + A_- (A_- - 1 + e) r v(t) \\ & \times u(t) - (A_- - 1 + e) v(t)], \quad (\text{A.7}) \\ v(t+1) = & e^{r(1-u(t))} [-B_+ r v(t) u(t) + B_+ v(t) \\ & - (B_- - 1 + e) u(t)], \end{aligned}$$

where the parameters A_+ , A_- , B_+ , and B_- are given by

$$A_+ = 1 - e + me[K_1^2(t) + K_2^2(t)]/[2K_1(t)K_2(t)],$$

$$A_- = 1 - e + me[K_1^2(t) - K_2^2(t)]/[2K_1(t)K_2(t)],$$

$$B_+ = 1 - e - me[K_1^2(t) + K_2^2(t)]/[2K_1(t)K_2(t)],$$

$$B_- = 1 - e - me[K_1^2(t) - K_2^2(t)]/[2K_1(t)K_2(t)].$$

Since the patches are non-identical, the synchronization state is now defined by $N_1/K_1 = N_2/K_2$. In addition, the variable v also appears in the equation for u . If the patches are nearly identical, i.e. $K_1(t) \approx K_2(t)$, eqn (A.7) can further be reduced, as follows. Let $K_1(t) \equiv K(t)$ and $K_2(t) = K(t) + \delta(t)$, where $\delta(t)$ is small compared to $K(t)$. In this case, after neglecting terms of order δ^2 or higher, we obtain

$$A_+ \approx 1 - e + me,$$

$$A_- \approx 1 - e - me\delta(t)/[K(t) + \delta(t)],$$

$$B_+ \approx 1 - e - me,$$

$$B_- \approx 1 - e + me\delta(t)/[K(t) + \delta(t)].$$

Thus, we have

$$\begin{aligned} u(t+1) &= e^{r(1-u(t))} \left[Au(t) + \frac{me\delta(t)rv(t)u(t)}{K(t) + \delta(t)} \right. \\ &\quad \left. + \frac{me\delta(t)v(t)}{K(t) + \delta(t)} \right], \\ v(t+1) &= e^{r(1-u(t))} \left[-Brv(t)u(t) + Bv(t) \right. \\ &\quad \left. + \frac{me\delta(t)u(t)}{K(t) + \delta(t)} \right]. \end{aligned} \quad (\text{A.8})$$

Since $\delta(t)$ is small, the last two terms in the $u(t+1)$ and $v(t+1)$ equations can be considered a small amplitude, additive random noise on the synchronization. Bifurcation diagrams similar to those in Fig. A3 are shown in Fig. A6, where we see that, compared with the identical patch case, the synchronization state is broadened and the parameter range for on-off intermittency increases. In fact, in the synchronization regime, as the difference between K_1 and K_2 increases, the synchronization state starts to develop a

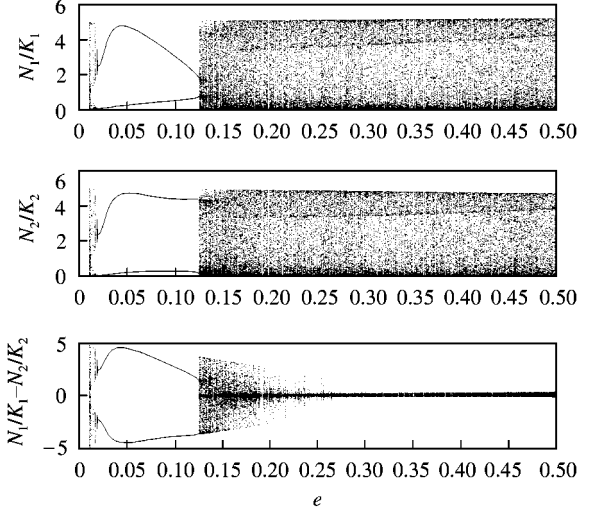


FIG. A6. Bifurcation diagrams for the one-clone, two non-identical patch model. Parameters values are $K_1 = \text{ran}[100, 110]$ (a uniform, random distribution between 110 and 110), $K_2 = \text{ran}[110, 120]$, $r = 4.0$, and $m = 1$.

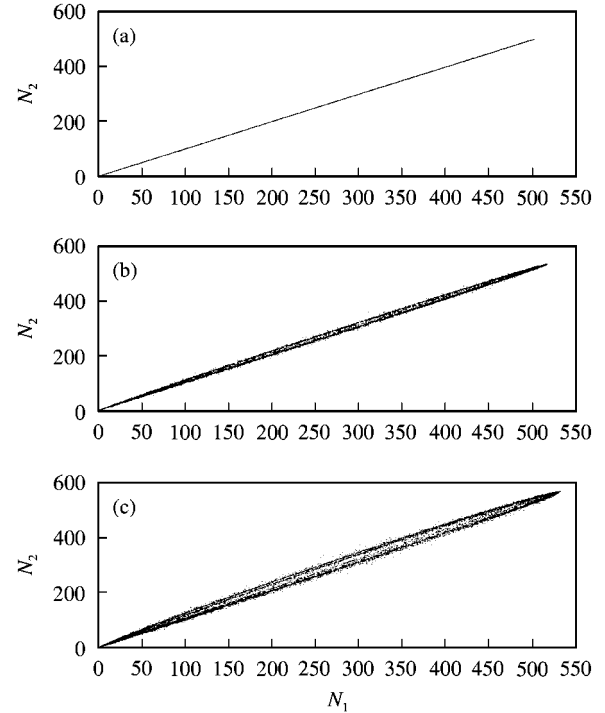


FIG. A7. The ellipsoid-like synchronization state in the one-clone, two non-identical patch models. (a) $K_1 = K_2 = \text{ran}[100, 110]$ (a uniform, random distribution between 100 and 110), (b) $K_1 = \text{ran}[100, 110]$, $K_2 = \text{ran}[110, 120]$, (c) $K_1 = \text{ran}[100, 110]$, $K_2 = \text{ran}[120, 130]$. Other parameters are $e = 0.3$, $m = 1$, and $r = 4$.

fractal-like band structure, as shown in Fig. A7(a–c). Study of the geometric structure of the synchronization manifold in coupled, non-identical systems is a forefront problem in chaotic dynamics (Barreto *et al.*, 2000).

CHAOS OR STOCHASTICITY?

As we have seen, under the presence of random perturbation in the model, as characterized by the noisy carrying capacities $K_1(t)$ and $K_2(t)$, intermittently chaotic synchronization can still be expected, which implies coexistence. We stress that the key requirement for species coexistence in a spatially extended environment is *temporal variation*. The form of temporal variation can be either random, chaotic, or a combination of both. For the models treated in this paper, chaos is the leading cause of the required temporal variation.

For ecological systems described approximately by these models, it can be concluded that chaotic synchronization is a general feature for dispersing species to coexist. One can also imagine the presence of a large amount of noise so that the system is essentially stochastic. In such a case, species coexistence can still be expected (Hastings, 1983; Holt, 1985), although now the leading cause is randomness rather than chaos. When a model is available, it is straight-forward to identify the origin of temporal variations, whether chaotic or stochastic. In a realistic situation as in laboratory or field experiments, a mathematical model is usually not available. In such a case, time series can be measured and the origin of temporal variation, i.e. stochasticity vs. chaos, can be assessed by utilizing existing techniques in nonlinear time-series analysis (for example, Sugihara & May, 1990; Kaplan, 1994; Stone *et al.*, 1996).